

Received January 27, 2019, accepted February 15, 2019, date of publication February 20, 2019, date of current version March 7, 2019.

Digital Object Identifier 10.1109/ACCESS.2019.2900323

Single Image Snow Removal via Composition Generative Adversarial Networks

ZHI LI¹, JUAN ZHANG¹, ZHIJUN FANG¹, (Senior Member, IEEE),
BO HUANG¹, XIAOYAN JIANG¹, YONGBIN GAO¹, AND
JENQ-NENG HWANG², (Fellow, IEEE)

¹Shanghai University of Engineering Science, Shanghai 201620, China

²University of Washington, Seattle, WA 98195, USA

Corresponding author: Juan Zhang (zhang-j@foxmail.com)

This work was supported by the National Natural Science Foundation of China under Grant 61702322, Grant 61772328, and Grant 61801288.

ABSTRACT Snowflakes attached to the camera lens can severely affect the visibility of the background scene and compromise the image quality. In this paper, we solve this problem by visually removing snowflakes to convert the snowy image into a clean one. The problem is troublesome; the information about the background of the occluded regions is completely lost for the most part. For removing snowflakes from a single image, we proposed a composition generative adversarial network. Different from the previous generative adversarial networks, our generator network comprises clean background module and a snow mask estimate module. The clean background module aims to generate a clear image from an input snowy image, and snow mask estimate module is used to produce the snow mask in an input image. During the training step, we put forward a composition loss between the input snowy image and composition of the generated clean image and estimated snow mask. We use a dataset named Snow100K² including indoor and outdoor scenes to train and test the proposed method. The extensive experiments on both synthetic and real-world images show that our network has a good effect and it is superior to the other state-of-the-art methods.

INDEX TERMS Remove snowflakes, composition generative adversarial network, dataset.

I. INTRODUCTION

With the progress in artificial intelligence, high-tech applications for various outdoor scenarios continue to emerge, such as automated driving systems and traffic monitoring. In most cases, the input images fed into these applications handling image-related tasks need to be sharp and clean so that the correct information can be extracted and processed. In practice, however, interferences are difficult to avoid, and they lead to degradation of the acquired images, poor visual effect, and less useful information in the images. Such images do not lead to satisfactory results after processing. Among various weather interferences, fog, rain, and snow are the most common. The study of image enhancement is therefore valuable for applications used for outdoor scene images.

Existing research on image enhancement mainly falls into two types: model based and machine learning based. The first type mainly uses traditional models to characterize texture and background image separately and transforms the entire

process into an iterative procedure through an appropriate optimization algorithm to obtain solutions. The latter type constructs a network architecture for image enhancement.

Kang *et al.* [1] proposed the use of a bilateral filter to decompose an image into high- and low-frequency components. The low-frequency component essentially retains most information concerning the background image, while the high-frequency component mainly contains the texture information and rain streaks. The histogram of oriented gradient (HOG) feature descriptors are applied on the high-frequency component. Dictionary-learning-based sparse coding is then used to extract the texture information of the background image from the high-frequency component, which, together with the low-frequency component, provides a final estimation of the background image. The idea behind this method, though intriguing, yields ambiguous results. Chen and Hsu [2] suggested the separation of rain streaks and background image from a rain image via discriminative sparse coding. Experiments demonstrated that clear estimated background images were obtained, but the rain streak removal effect was less than satisfactory. As research advances and

The associate editor coordinating the review of this manuscript and approving it for publication was Yuming Fang.

the understanding of actual rainy images deepens, researchers have found the formation of fog in different degrees along with the rain; this also affects the visual effect of the estimated background image. Based on patch-based learning, Li *et al.* [3] used Gaussian mixture models to characterize the priors of background and rain layers. The validity of this method in actual rain removal was proven in their study concerning the joint use of the defogging algorithm. By far, this method produces the best result among all the models described, but some missing details from the estimated background image leads to image blurring.

Compared to the application of models in image enhancement, the research on deep learning architecture for image enhancement has just emerged in recent years. Fu *et al.* [4] proposed a network architecture called DerainNet based on a deep convolutional neural network. In addition, considering the effect of fog caused by the rain, they suggested the performance of defogging after rain removal. In addition, Fu *et al.* simplified the learning mode of deep residual networks and proposed a deep detailed network to tackle deraining. The processing capacity of this network architecture was validated by use in denoising and other processes. Yang *et al.* [5] suggested the detection of rain streak locations in rain images and varied the degrees of removal according to different intensities of the rain streaks. A multi-task deep network is, in this case, designed to carry out the detection and removal iteratively. They [6] also took into account the impact of fog on visual perception and attempted to employ a joint deraining-defogging-deraining methodology to eliminate rain and fog. Experiments indicated that their method is particularly effective for heavy rain.

In these image enhancement tasks, factors such as the varied size and shape of snowflakes and irregular trajectory make snow removal from the image even more challenging. Liu *et al.* [7] designed DesnowNet to deal with this problem, and it has proved to be effective experimentally.

In order to solve the snow removal problem, this paper proposes a novel method - composition generative adversarial networks (CGAN), which can effectively remove the snowflakes in the image under different snow particle sizes (see Figure 1).

The contribution of this paper are as follows: 1) This paper proposed a novel snow removal algorithm based on generative adversarial networks (GAN) called CGAN. The CGAN include generator network and discriminator network. 2) In the generator network, we use the new structure based on encoder-decoder architecture, it consists of clean background module and snow mask estimate module. 3) We develop an up-to-date loss function based on least squares loss, mean absolute error (MAE) loss and composition loss.

II. RELATED WORKS

In this section, we briefly review the existing deep-learning based single image snow removal algorithms, and the development of GAN.



FIGURE 1. Sample results of our method. From left to right: Real world snowy images, pristine images.

A. SINGLE IMAGE SNOW REMOVAL

Single image snow removal is used to restore a clear image from a snowy image which is corrupted by snowflakes. This relationship can be formulated by [7]

$$I = J \odot m + A \odot (1 - m) \quad (1)$$

where I represents snowy images, A is the clear image, m is the snow masks, J is the chromatic aberration map, and \odot denotes element-wise multiplication.

Due to the success of convolutional neural networks (CNN) in classification and recognition [8]–[10], it has been applied in the snow removal. Liu *et al.* [7] proposed a network architecture called DesnowNet based on a multistage convolutional neural network. It first estimates the snow mask and aberration map by CNN, then uses a conventional method to recover clear images. However, DesnowNet has poor robustness to real world snowy images. Thus, we present a novel method for snow removal.

B. GENERATIVE ADVERSARIAL NETWORK

To generate realistic-looking images, in 2014, Goodfellow *et al.* [11] proposed the GAN framework. GAN consists of a generator network and a discriminator network.

The generator network is used to generate image from input image and the discriminator network aims to distinguish whether the generated image is from real data or the generator network. However, GAN is not stable in the training process and often produces artifacts such as noise and color shift in the generated images [12]. Arjovsky *et al.* [12] discussed the difficulties in GAN training caused by JS divergence approximation and proposed to use the Earth-Mover’s (also called Wasserstein-1) distance $W(q, p)$. Furthermore, Mao *et al.* [13] proposed the least squares generative adversarial networks (LSGANs) which adopt the least squares loss function for the discriminator to overcome mode collapse, vanishing gradient, etc. in the training process.

Recently, GAN has received increased attention. It has been applied to different image-to-image translation problems, such as style transfer [14], [15], photo enhancement [16], super resolution [17], and others [18]–[20].

III. PROPOSED METHOD

In this section, we introduce the network architecture of the CGAN including the generator and the discriminator. In the following, we present loss function in details and show the results of the snow mask estimate module.

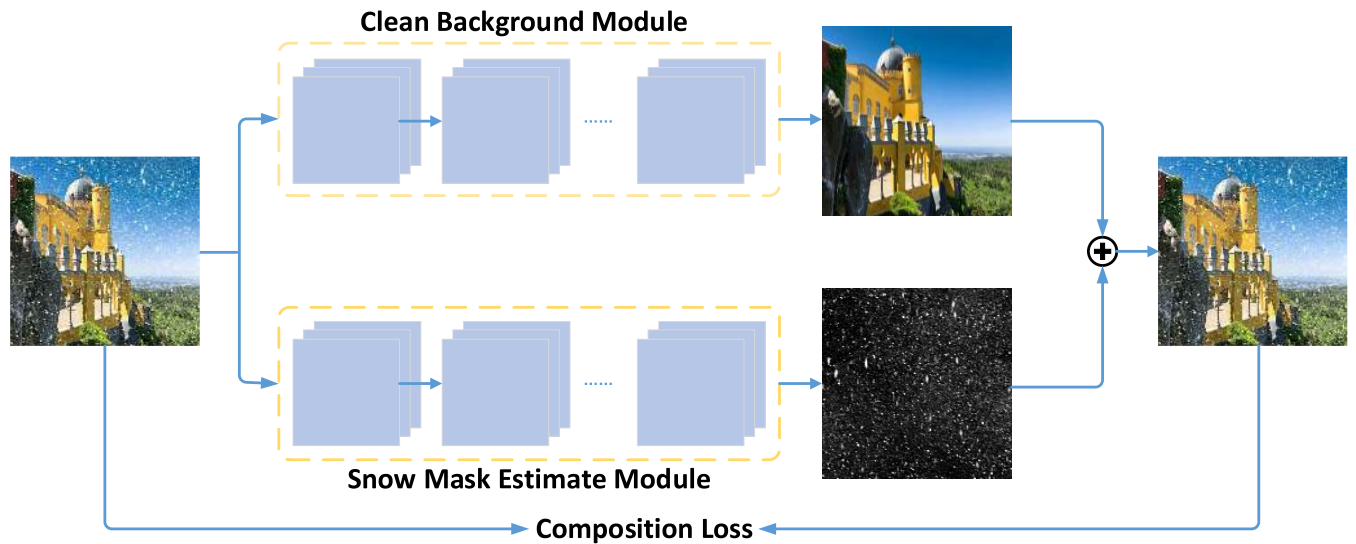


FIGURE 2. Architecture of our proposed generator network. It consists of a clean background module and a snow mask estimate module.

TABLE 1. Architecture of the clean background module and parameter setting. “conv” denotes the convolution, “uconv” denotes the deconvolution.

Encoding	Layer	conv	conv	conv	conv	conv	conv	conv	conv	conv	conv	
	Kernel	5×5	3×3	4×4	4×4	4×4	4×4	4×4	4×4	4×4	4×4	
	Stride	1×1	1×1	2×2	2×2	2×2	2×2	2×2	2×2	2×2	2×2	
	Channel	64	64	64	128	256	512	1024	1024	1024	1024	
Decoding	Layer	uconv	uconv	uconv	uconv	uconv	uconv	uconv	uconv	conv	Tanh	
	Kernel	4×4	4×4	4×4	4×4	4×4	4×4	4×4	4×4	3×3	-	
	Stride	2×2	2×2	2×2	2×2	2×2	2×2	2×2	2×2	1×1	-	
		Channel	1024	1024	1024	512	256	128	64	64	3	-

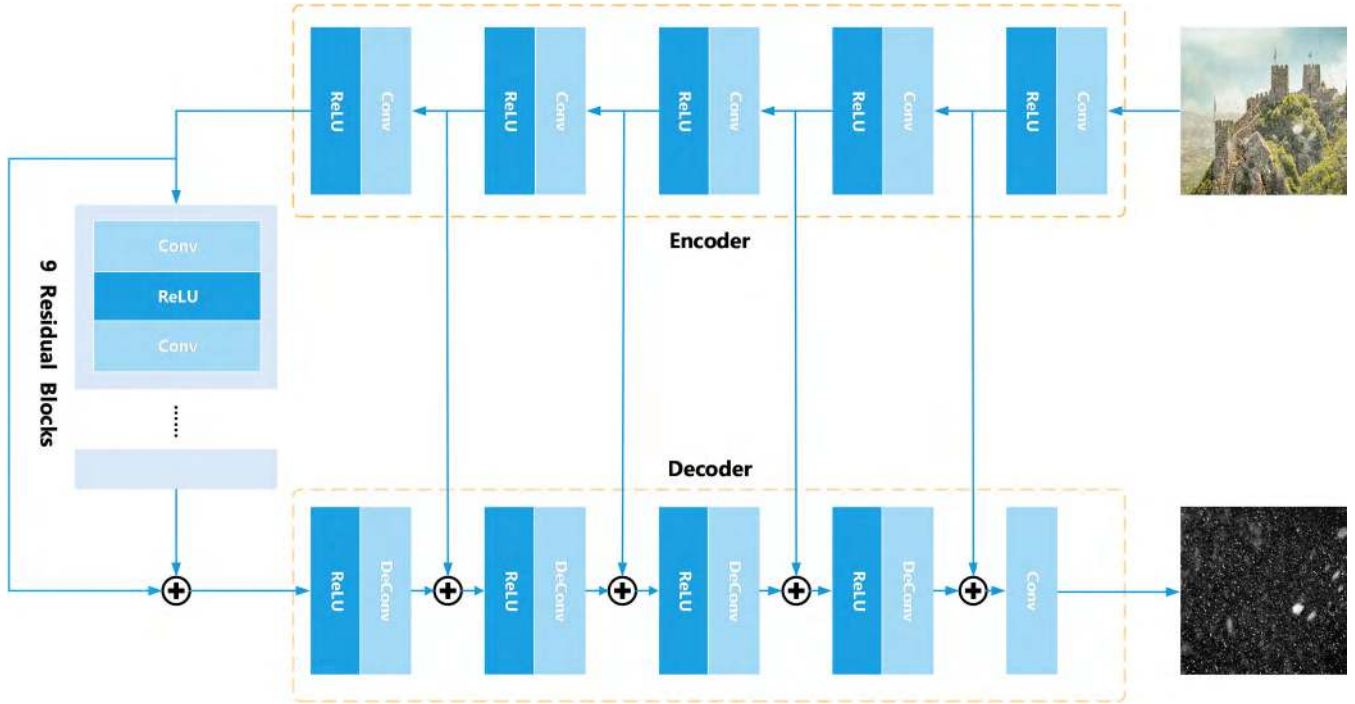


FIGURE 3. Architecture of the snow mask estimate module.

nine residual blocks (ResBlock) [21] and four transposed convolution blocks. Each ResBlock consists of a convolution layer, an instance normalization layer [22], and a ReLU activation layer [23]. Dropout [24] with probability of 0.5 is added to the generator after the first convolution layer in each ResBlock [21]. The sample results of the snow mask estimate module as shown in Figure 4. The loss function of pre-trained snow mask estimate module can be written as:

$$L_E = \frac{1}{N} \sum_{i=1}^N \|z - M(x)\|_2^2 \quad (2)$$

where N stand for the number of training images, x is the input snowy image, z is the corresponding snow mask and function $M(\blacksquare)$ is used to generate snow mask.

B. DISCRIMINATOR NETWORK

The discriminator network is used to classify whether a pair of images is real (1) or fake (0). The proposed discriminator network as shown in Figure 5 contains a heap of convolutional layers, where each convolutional layer is followed by a batch normalization layer and LeakyReLU activation layer. The last layer of the discriminator network is a sigmoid function, which outputs the probability of the input image pair to be real or fake.

C. LOSS FUNCTION

We formulate the loss function as the weighted sum of least squares loss [13], MAE loss and composition loss as:

$$L = \alpha L_{ls} + \beta L_1 + \gamma L_C \quad (3)$$

1) LEAST SQUARES LOSS

Most of the papers related to GANs, use vanilla GANs objective as a loss. However, we find that the CGAN using this loss is not able to remove the snow well and also product some artifacts and color shift on generated snowy images. As shown in the following, the quantitative results (Table 3) indicate that only using vanilla GANs objective does not generate clear images. Therefore, we use least squares loss as the critic function. the loss is calculated as the following:

$$L_{ls} = \mathbb{E}_{x,y \sim P_{data(x,y)}} \left[(D(x,y) - b)^2 \right] + \mathbb{E}_{x \sim P_{data(x)}} \left[(D(x, C(x)) - a)^2 \right] \quad (4)$$

where x is the input snowy image, y denotes the ground truth snow-free image, $C(\blacksquare)$ is the function of generate clean image and $D(\blacksquare)$ is the function of discriminator, the setting of a and b which represents the labels indicating whether the sample is real will be described in section IV (B).

2) MAE LOSS

The benefit of using MAE loss is that it encourages the clean background module to generate images which are closer to ground truth images. The MAE loss between ground-truth snow-free image y and the generated snow-free image $C(x)$ is given by:

$$L_{MAE} = \frac{1}{N} \sum_{i=1}^N \|y - C(x)\|_1 \quad (5)$$



FIGURE 4. Example results of the snow mask estimate module. From top to bottom: Input snowy images, generated snow masks, ground truth.



FIGURE 5. The architecture of the proposed discriminator network.

3) COMPOSITION LOSS

In order to remove the artifacts and color shift of the generated snowy image, we introduce composition loss helps to minimize pixel-level differences between input snowy image x and composition of the generated clean image $C(x)$ and estimated snow mask $M(x)$, which is defined as:

$$L_C = \frac{1}{N} \sum_{i=1}^N \|x - (C(x) + M(x))\|_1 \quad (6)$$



FIGURE 6. Sample image of Snow100K². From top to bottom: Sample synthetic snowy images, ground truth and corresponding snow masks.

IV. EXPERIMENTS

In this section, we first introduce the dataset and training details of our method. In the following, this paper further analyzes and discuss the effect of the proposed algorithm including the discriminator architecture and loss function. Finally, we discuss the application of the proposed method.

A. DATASET

In this study, a large-scale dataset named Snow100K² [7] was used for testing and training. It consisted of 1) 100,000 synthesized snowy images, 2) the corresponding snow-free images, and 3) snow masks. The snow-free images were captured using Flickr API [25]. To synthesize snow images, Liu et al. [7] use Photoshop to create 5,800 masks. Each mask contained snowflakes of different shapes. Corresponding examples are shown in Figure 6 and the number of training and testing set introduced in Table 2.

B. TRAINING DETAILS

We train the network on an NVIDIA 1080Ti GPU. The proposed method is implemented using the TensorFlow 1.10.0 [26] and Python 3.6.0. Each layer of the proposed generator network consists of a convolution, instance normalization [22] and LeakyReLU. All the training images are resized to 256×256 . We set the parameters of batch-size, initial learning rate for Adam, and momentum to 1, 0.0002, and 0.5, respectively. Training stage stops at 200 epochs. The parameters are initialized as follows: $\alpha = 1, \beta = 50, \gamma = 50, a = 1, b = 0$. As same as vanilla GAN, the generator network and the discriminator network are alternately updated.

TABLE 2. Number of each subset of Snow100K² dataset.

Subset	Snow100K-S	Snow100K-M	Snow100K-L
Training	16643	16622	16735
Testing	16611	16588	16801

C. EFFECT OF THE LOSS FUNCTION IN CGAN

Introduction through section III, we advance a new loss function, which consists of least squares loss, MAE loss and composition loss. In the following, this paper will demonstrate the validity of this loss function through experiments.

1) ADVERSARIAL LOSS VS. LEAST SQUARES LOSS

In order to confirm the effectiveness of least squares loss, we train the least squares loss [13] and adversarial loss [11] under the same network and use average PSNR and SSIM to evaluate the results separately. It can be seen in Table 2 that the least squares loss function gets higher PSNR value. Therefore, the proposed algorithm uses least squares loss.

2) EFFECT OF THE COMPOSITION LOSS

In order to verify the effectiveness of our loss function, we experimented different loss functions under the same condition. It can be seen in Table 3 that the proposed loss function generates better results. We note that the method with $L_{ls} + L_c$ loss generates the results with higher PSNR values compared with the method with $L_{ls} + L_{MAE}$ loss. The results from the second column and the third column show that L_{MAE} helps to improve the SSIM value, and indicate that it is able to preserve the structures of images. Figure 7 shows some snow

removal results examples with different loss functions and corresponding PSNR/SSIM. The method with the proposed loss function generates better results.

D. DIFFERENT ARCHITECTURE OF DISCRIMINATOR NETWORK

For purpose of prove the effectiveness of our discriminator network, we experimented and evaluated different architecture of the discriminator. The experimental settings of the discriminator are listed below:

- 1 × 1 PixelGAN discriminator:** The 1 × 1 PixelGAN discriminator structure is: C64 – C128. In this case, each layer is 1 × 1 filter size.
- 16 × 16 PatchGAN discriminator:** The 16 × 16 PatchGAN discriminator architecture is: C64 – C128.
- 70 × 70 PatchGAN discriminator:** The 70 × 70 PatchGAN discriminator architecture is: C64 – C128 – C256 – C512.
- 286 × 286 ImageGAN discriminator:** In this special case, input image first resized to 286 × 286. The 286 × 286 ImageGAN discriminator architecture is: C64 – C128 – C256 – C512 – C512 – C512,

where C denotes the output channel. Figure 8 shows three real snowy images and the corresponding snow removal

TABLE 3. Quantitatively evaluate the effect of the different loss functions in the proposed method.

Loss	L_{ad}	L_{ls}	$L_{ls} + L_{MAE}$	$L_{ls} + L_c$	$L_{ls} + L_{MAE} + L_c$
PSNR	27.4523	28.2513	28.4634	29.3421	30.3972
SSIM	0.9067	0.9132	0.9171	0.9232	0.9355



FIGURE 7. The effect of the proposed network with different loss function. (c) L_{ad} loss. (d) L_{ls} loss. (e) $L_{ls} + L_{MAE}$ loss. (f) $L_{ls} + L_c$ loss (g) $L_{ls} + L_{MAE} + L_c$ loss.

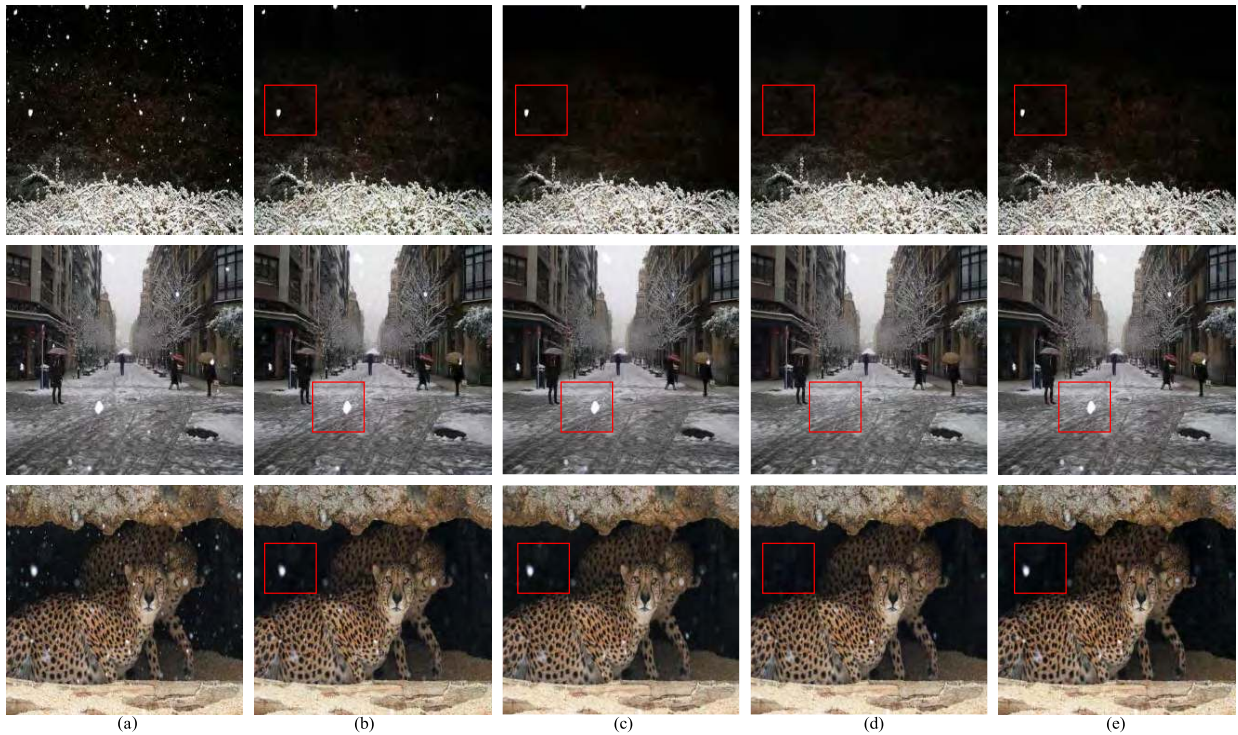


FIGURE 8. The effect of the different architecture of discriminator network. (a) Input image. (b) 1×1 . (c) 16×16 . (d) 70×70 . (e) 286×286 .

results generated by CGAN with different architecture of discriminator network, 70×70 PatchGAN discriminator generates better results. The other is able to remove some snowflakes, but the recovered images still contain snow partials and some artifacts. Therefore, the proposed discriminator network use 70×70 PatchGAN architecture.

E. APPLICATION

To provide further evidence that our image enhancement could be beneficial for computer vision recognition, we employ YOLO-V3 [27] to test our method. The results are shown in Figure 9. As can be seen, using our output image, the general recognition is better than the one without our image enhancement process.

V. COMPARISON

In this section, we compare our approach with the other state-of-the-art methods on synthetic dataset and real-world snowy images.

A. QUANTITATIVE ANALYSIS

We compare quantitative performance of different methods on the test images from the synthetic snowy image dataset,



FIGURE 9. Sample result of YOLO-V3. From left to right: Real world snowy image, generated clean image.

Snow100K². Quantitative results corresponding to different methods are tabulated in Table 4. It can be clearly observed that the proposed method is able to achieve superior quantitative performance.

B. REAL IMAGE SNOW REMOVAL

The snow removal effect of the proposed method was evaluated using five real-world snow scene images. The removal outcomes are presented in Figure 10. The snow removal results of DesnowNet [7] show that the first and second images were over-processed. In the second image,

TABLE 4. Respective performances of the state-of-the-art method evaluated via Snow100K²'s test set.

Subset	Snow100K-S		Snow100K-M		Snow100K-L		Overall	
	PSNR	SSIM	PSNR	SSIM	PSNR	SSIM	PSNR	SSIM
DesnowNet	32.3331	0.95	30.8682	0.9409	27.1699	0.8983	30.1121	0.9296
Ours	30.4326	0.9612	31.2103	0.9431	29.5487	0.9021	30.3972	0.9355



FIGURE 10. Real world snowy images and results from state-of-the-art methods. From left to right: Input real world snowy images, results of DesnowNet, results of our method.

the distant lights were removed as snowflakes by DesnowNet. However, snow was not completely removed in the other three images. Our method led to clearer visual representations than DesnowNet did. As seen in the first image, our method yielded more refined processing results.

VI. CONCLUSION

In this work, we introduce a novel deep learning snow removal algorithm based on GAN. Our approach was fully different from existing snow removal methods which focus on estimating the snow mask and aberration map from the input snowy image and then use conventional method to recover clear image. To generate better results, we have proposed a multistage network including clean background module and snow mask estimate module, therefore, it can capture more useful information. We further modify the basic GAN formulation by advancing new loss function to generate clear images. The proposed method performs favorably against several state-of-the-art methods on both synthetic dataset and real-world snowy images.

REFERENCES

- [1] L.-W. Kang, C.-W. Lin, and Y.-H. Fu, "Automatic single-image-based rain streaks removal via image decomposition," *IEEE Trans. Image Process.*, vol. 21, no. 4, pp. 1742–1755, Apr. 2012.
- [2] Y.-L. Chen and C.-T. Hsu, "A generalized low-rank appearance model for spatio-temporally correlated rain streaks," in *Proc. IEEE Int. Conf. Comput. Vis. (ICCV)*, Dec. 2013, pp. 1968–1975.
- [3] Y. Li, R. T. Tan, X. Guo, J. Lu, and M. S. Brown, "Rain streak removal using layer priors," in *Proc. IEEE Conf. Comput. Vis. Pattern Recognit. (CVPR)*, Jun. 2016, pp. 2736–2744.
- [4] X. Fu, J. Huang, X. Ding, Y. Liao, and J. Paisley, "Clearing the skies: A deep network architecture for single-image rain removal," *IEEE Trans. Image Process.*, vol. 26, no. 6, pp. 2944–2956, Jun. 2017.
- [5] W. Yang, R. T. Tan, J. Feng, J. Liu, Z. Guo, and S. Yan, "Deep joint rain detection and removal from a single image," in *Proc. IEEE Conf. Comput. Vis. Pattern Recognit. (CVPR)*, Jun. 2017, pp. 1357–1366.
- [6] X. Fu, J. Huang, D. Zeng, Y. Huang, X. Ding, and J. Paisley, "Removing rain from single images via a deep detail network," in *Proc. IEEE Conf. Comput. Vis. Pattern Recognit. (CVPR)*, Jul. 2017, pp. 1715–1723.
- [7] Y.-F. Liu, D.-W. Jaw, S.-C. Huang, and J.-N. Hwang, "DesnowNet: Context-aware deep network for snow removal," *IEEE Trans. Image Process.*, vol. 27, no. 6, pp. 3064–3073, Jun. 2018.
- [8] J. Long, E. Shelhamer, and T. Darrell, "Fully convolutional networks for semantic segmentation," in *Proc. IEEE Conf. Comput. Vis. Pattern Recognit. (CVPR)*, Jun. 2015, pp. 3431–3440.
- [9] O. Ronneberger, P. Fischer, and T. Brox, "U-Net: Convolutional networks for biomedical image segmentation," in *Proc. Int. Conf. Med. Image Comput. Comput.-Assist. Intervent.* Cham, Switzerland: Springer, 2015, pp. 234–241.
- [10] K. He, G. Gkioxari, P. Dollár, and R. Girshick, "Mask R-CNN," in *Proc. IEEE Conf. Comput. Vis. (ICCV)*, Oct. 2017, pp. 2980–2988.
- [11] I. Goodfellow et al., "Generative adversarial nets," in *Proc. Adv. Neural Inf. Process. Syst. (NIPS)*, 2014, pp. 2672–2680.
- [12] M. Arjovsky, S. Chintala, and L. Bottou. (2017). "Wasserstein GAN." [Online]. Available: <https://arxiv.org/abs/1701.07875>
- [13] X. Mao, Q. Li, H. Xie, R. Y. K. Lau, Z. Wang, and S. P. Smolley, "Least squares generative adversarial networks," in *Proc. IEEE Int. Conf. Comput. Vis. (ICCV)*, Oct. 2017, pp. 2813–2821.
- [14] H. Chang, J. Lu, F. Yu, and A. Finkelstein, "PairedCycleGAN: Asymmetric style transfer for applying and removing makeup," in *Proc. IEEE Conf. Comput. Vis. Pattern Recognit. (CVPR)*, 2018, pp. 40–48.
- [15] Y. Choi, M. Choi, M. Kim, J.-W. Ha, S. Kim, and J. Choo, "StarGAN: Unified generative adversarial networks for multi-domain image-to-image translation," in *Proc. IEEE Conf. Comput. Vis. Pattern Recognit. (CVPR)*, Jun. 2018, pp. 8789–8797.
- [16] Y.-S. Chen, Y.-C. Wang, M.-H. Kao, and Y.-Y. Chuang, "Deep photo enhancer: Unpaired learning for image enhancement from photographs with GANs," in *Proc. IEEE Conf. Comput. Vis. Pattern Recognit. (CVPR)* 2018, pp. 6306–6314.
- [17] C. Ledig et al., "Photo-realistic single image super-resolution using a generative adversarial network," in *Proc. IEEE Conf. Comput. Vis. Pattern Recognit. (CVPR)*, Jul. 2017, pp. 105–114.
- [18] A. Bulat and G. Tzimiropoulos, "Super-FAN: Integrated facial landmark localization and super-resolution of real-world low resolution faces in arbitrary poses with GANs," in *Proc. IEEE Conf. Comput. Vis. Pattern Recognit. (CVPR)*, Jun. 2018, pp. 109–117.
- [19] A. Gupta, J. Johnson, L. Fei-Fei, S. Savarese, and A. Alahi, "Social GAN: Socially acceptable trajectories with generative adversarial networks," in *Proc. IEEE Conf. Comput. Vis. Pattern Recognit. (CVPR)*, Jun. 2018, pp. 2255–2264.
- [20] W. Deng, L. Zheng, Q. Ye, G. Kang, Y. Yang, and J. Jiao, "Image-image domain adaptation with preserved self-similarity and domain-dissimilarity for person re-identification," in *Proc. IEEE Conf. Comput. Vis. Pattern Recognit. (CVPR)*, 2018, pp. 994–1003.
- [21] K. He, X. Zhang, S. Ren, and J. Sun, "Deep residual learning for image recognition," in *Proc. IEEE Conf. Comput. Vis. Pattern Recognit. (CVPR)*, Jun. 2016, pp. 770–778.
- [22] D. Ulyanov, A. Vedaldi, and V. Lempitsky. (2016). "Instance normalization: The missing ingredient for fast stylization." [Online]. Available: <https://arxiv.org/abs/1607.08022>
- [23] A. Krizhevsky, I. Sutskever, and G. E. Hinton, "ImageNet classification with deep convolutional neural networks," in *Proc. Adv. Neural Inf. Process. Syst. (NIPS)*, 2012, pp. 1097–1105.
- [24] N. Srivastava, G. Hinton, A. Krizhevsky, I. Sutskever, and R. Salakhutdinov, "Dropout: A simple way to prevent neural networks from overfitting," *J. Mach. Learn. Res.*, vol. 15, no. 1, pp. 1929–1958, 2014.
- [25] [Online]. Available: <https://www.flickr.com/services/api/>
- [26] [Online]. Available: <https://tensorflow.google.cn/>
- [27] J. Redmon and A. Farhadi. (2018). "YOLOV3: An incremental improvement." [Online]. Available: <https://arxiv.org/abs/1804.02767>



ZHI LI received the B.S. degree in computer science from the Suzhou University of Science and Technology. He is currently pursuing the M.S. degree in the field of traffic engineering with the Shanghai University of Engineering Science. His research interests include image processing and deep learning.



JUAN ZHANG received the B.S. and M.S. degrees in computer science from Jiangxi Normal University, China, in 1997 and 2005, respectively, and the Ph.D. degree in computer science from Shanghai University, China, in 2012. She is currently an Associate Professor with the School of Electronic and Electrical Engineering, Shanghai University of Engineering Science, China. Her research interest includes computer vision.



ZHIJUN FANG received the Ph.D. degree from Shanghai Jiao Tong University, Shanghai, China. He is currently a Professor and the Dean of the School of Electronic and Electrical Engineering, Shanghai University of Engineering Science. His current research interests include image processing, video coding, and pattern recognition. He was a recipient of the GanPo 555 Talents Program Award, and the One-Hundred, the One-Thousand, and the Ten-Thousand Talent Project Award of Jiangxi Province. He was the General Chair of the Joint Conference on Harmonious Human Machine Environment 2013 and a General Co-Chair of the International Symposium on Information Technology Convergence, from 2014 to 2017.



BO HUANG received the Ph.D. degree from Wuhan University, China, in 2014. He is currently a Lecturer with the School of Electronic and Electrical Engineering, Shanghai University of Engineering Science, China. His research interests include artificial intelligence and software engineering.



XIAOYAN JIANG received the Ph.D. degree in computer science from the Friedrich-Schiller University of Jena, Jena, Germany. She is currently a Lecturer with the School of Electronic and Electrical Engineering, Shanghai University of Engineering Science, Shanghai, China. She has published numerous SCI/EI papers in the field of computer vision. Her research interests include sensor data fusion, multi-object tracking for autonomous driving and visual surveillance, probability theory, and optimization algorithms. She received the fund from the National Natural Science Foundation of China, in 2017, and scholarships from the Chinese Government and the German Academic Exchange Service (DAAD).



YONGBIN GAO received the Ph.D. degree from Chonbuk National University, South Korea. He is currently a Faculty Member with the School of Electronic and Electrical Engineering, Shanghai University of Engineering Science, Shanghai, China. He has published numerous SCI papers in prestigious journals, such as *Information Science Letters* and *Pattern Recognition Letters*, in the area of image processing, patter recognition, and computer vision.



JENQ-NENG HWANG (F'01) received the B.S. and M.S. degrees in electrical engineering from National Taiwan University, Taiwan, China, in 1981 and 1983, respectively, and the Ph.D. degree from the University of Southern California. In 1989, he joined the Department of Electrical Engineering, University of Washington, Seattle, where he has been a Full Professor, since 1999. He is currently a member of Multimedia Technical Committee of the IEEE Communication Society and the Multimedia Signal Processing Technical Committee of the IEEE Signal Processing Society. He is a Founding Member of the Multimedia Signal Processing Technical Committee of the IEEE Signal Processing Society. He was a recipient of the 1995 IEEE Signal Processing Society's Best Journal Paper Award. He was a Society's Representative of the IEEE Neural Network Council, from 1996 to 2000. He served as Associate Editor for IEEE T-SP, T-NN, T-CSVT, T-IP, and *Signal Processing Magazine*. He is on the Editorial Board of *ZTE Communications*, *ETRI*, *IJDMB*, and *JSPS* journals. He served as the Program Co-Chair for the IEEE ICME 2016. He was the Program Co-Chair of ICASSP 1998 and ISCAS 2009.

...